Disentangling electrical switching of antiferromagnetic NiO using high magnetic fields

C. F. Schippers,[1,*] M. J. Grzybowski,[1,†] K. Rubi,[2,‡] M. E. Bal,[2] T. J. Kools,[1] R. A. Duine,[1,3] U. Zeitler,[2] and H. J. M. Swagten[1]

[1]*Department of Applied Physics, Eindhoven University of Technology, P.O. Box 513, 5600 MB Eindhoven, The Netherlands*

[2]*High Field Magnet Laboratory (HFML-EMFL), Radboud University, 6525 ED Nijmegen, The Netherlands*

[3]*Institute for Theoretical Physics, Utrecht University, Leuvenlaan 4, 3584 CE Utrecht, The Netherlands*

(Received 12 April 2022; revised 27 October 2022; accepted 16 November 2022; published 28 November 2022)

Recent demonstrations of the electrical switching of antiferromagnets (AFs) have given an enormous impulse to the field of AF spintronics. Many of these observations are plagued by nonmagnetic effects that are very difficult to distinguish from the actual magnetic ones. Here, we study the electrical switching of thin (5 nm) NiO films in Pt/NiO devices using magnetic fields up to 15 T to quantitatively disentangle these magnetic and nonmagnetic effects. We demonstrate that these fields suppress the magnetic components of the electrical switching of NiO, but leave the nonmagnetic components intact. Using a monodomainization model the contributions are separated, showing how they behave as a function of the current density. These results show that combining electrical methods and strong magnetic fields can be an invaluable tool for AF spintronics, allowing for implementing and studying electrical switching of AFs in more complex systems.

DOI: 10.1103/PhysRevB.106.174434

I. INTRODUCTION

Recently, there has been a lot of attention paid for controlling the magnetic order of antiferromagnetic materials. The insensitivity to external magnetic fields, combined with THz-frequency magnetization dynamics, makes antiferromagnets interesting for numerous applications, ranging from data-storage devices [1] to THz radiation sources [2–4]. However, control over the orientation of the magnetic order in an antiferromagnet remains problematic and it has only recently been demonstrated that the magnetic order can be controlled using electrical currents [5,6]. Since these first demonstrations, there have been many experiments that manipulated the antiferromagnetic state in a variety of systems, such as multilayer systems with antiferromagnets and ferromagnets [7,8], or systems with noncollinear antiferromagnets [9,10].

In insulating antiferromagnets, such as NiO, CoO, and Fe_2O_3, experiments showed that the magnetic order can be controlled using electrical current pulses through an adjacent heavy metal (e.g., Pt) [6,11–13]. The current in the heavy metal layer is, via the spin-Hall effect, converted into a transverse spin current. In turn, this spin current is injected into the antiferromagnet where it exerts a spin torque on the spins, which is then expected to manipulate the magnetic order of the antiferromagnet [6,14]. Alternatively, Joule heating due to the current pulse can give rise to a thermomagnetoelastic effect, which can change the anisotropy of the antiferromagnet sufficiently to induce a change in the antiferromagnetic order [15].

However, recently there has been a debate about the actual origin of the signals observed in the above-mentioned electrical switching experiments, as they can equally well be explained by nonmagnetic, parasitic effects, such as structural changes or damage caused by Joule heating, or electromigration [12,16–18]. Although there are demonstrations that show with certainty that actual magnetic reorientation is possible, it is generally difficult to distinguish between the magnetic and nonmagnetic contributions to the electrical switching signals, as the electrical measurements themselves consist only of Hall measurements showing the electrically induced switching as an up-down pattern. This shortcoming can be resolved using imaging techniques that can resolve the magnetic state of an antiferromagnet, such as x-ray magnetic linear dichroism-photoemission electron microscopy (XMLD-PEEM) [14,19]. However, this requires an x-ray beamline and is limited to devices with relatively free access to the antiferromagnet in question, i.e., devices where the antiferromagnetic layer is not buried beneath other layers.

Here we disentangle magnetic and nonmagnetic effects in the electrical switching of thin films of NiO using strong magnetic fields of up to 15 T. If the magnetic field is stronger than the monodomainization field (determined to be (13.5 ± 0.2) T for our samples, see Supplemental Material [20] and also [21,22] therein) the magnetic order of NiO is organized in a single domain whose magnetic orientation is controlled by the external magnetic field [21]. Hence, the effect of reorienting the magnetic moments in an electrical switching experiment is expected to be suppressed in such a field. As Joule heating and electromigration are not affected by the magnetic field, they will therefore remain present, giving a way to disentangle the magnetic and nonmagnetic contributions.

*c.f.schippers@tue.nl

†Current address: Institute of Experimental Physics, Faculty of Physics, University of Warsaw, ul. Pasteura 5, PL-02-093 Warsaw, Poland.

‡Current address: National High Magnetic Field Laboratory, Los Alamos National Laboratory, Los Alamos, NM 87545, USA.

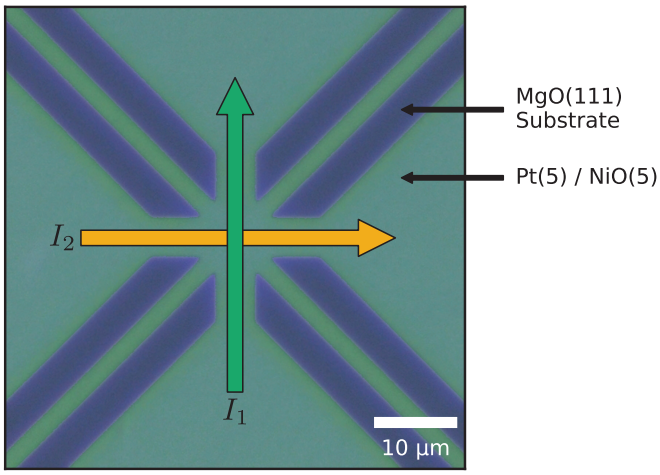

FIG. 1. Micrograph of the device used for the electrical switching experiments. It consists of Pt and NiO, each 5 nm thick, on top of an MgO(111) substrate. The green and orange arrows indicate the current pulse directions (I_1 and I_2); the two diagonal lines are used for the spin-Hall magnetoresistance measurements. Colors are enhanced for clarity.

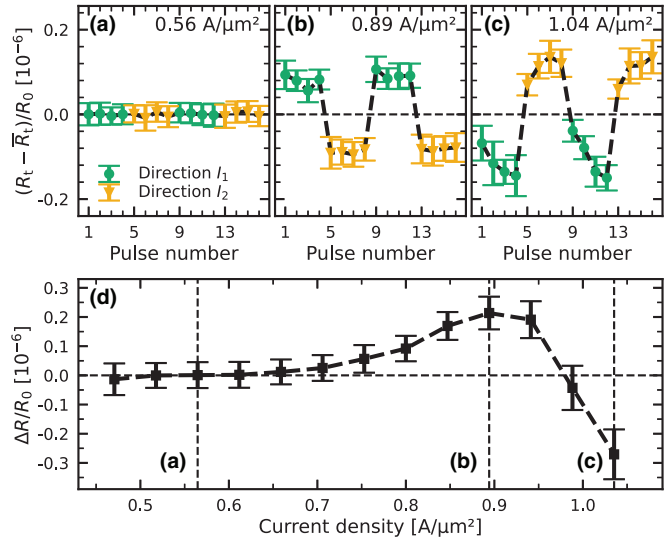

FIG. 2. Current dependence of electrical switching in zero field at 250 K. (a)–(c) show the measured transverse resistances (minus the average transverse resistance $\overline{R}_t$) after a current pulse for increasing pulse current densities (0.56 A/µm², 0.89 A/µm², and 1.04 A/µm², respectively). The green (orange) data points represent current pulses along direction I_1 (I_2). The shown data points are averages of four repeats of the full measurement cycle. (d) The current dependence of the switching amplitude (i.e., the difference between the average transverse resistance of the two orthogonal current pulse orientations) as a function of the pulse current density. All data are normalized by the longitudinal device resistance $R_0 = (1.76 \pm 0.04)\,\mathrm{k\Omega}$ and the black dashed lines are guides to the eye.

We show that it is indeed possible to suppress the electrical switching effects in Pt/NiO devices by applying a sufficiently strong magnetic field of over 13.5 T. Field dependence of the switching signal is observed and can be understood and modeled with a multidomain interpretation of the NiO magnetic structure [21]. Using this model, we demonstrate that the magnetic and nonmagnetic contributions to the observed switching signal can be separated from each other. Thereby, this technique helps to better understand the electrical switching experiments and allows integrating and investigating the electrical switching of antiferromagnets in more complex devices.

II. SAMPLES AND METHODS

For these experiments, we fabricate eight-terminal devices as shown in Fig. 1 consisting of NiO on top of a Pt layer (5 nm each) on MgO(111) substrates. Both layers are grown using DC magnetron sputtering, at 565° C for the Pt layer to ensure the crystallinity of the Pt layer and at 430° C in a 10 : 1 Ar:O-mixture for the NiO layer. The quality of these layers is ensured using a variety of characterization techniques (see Supplemental Material [20] and also [23–29] therein). From these layers, devices as shown in Fig. 1 are fabricated using a combination of electron-beam lithography, electron-beam evaporation, lift-off, and ion-beam milling.

With these devices electrical switching experiments are performed, similar to the ones discussed in the literature [6]. To switch the AF state, current pulses of 3 ms are applied along the wide orthogonal current lines I_1 and I_2, as indicated in Fig. 1 (the probe lines are also included when applying the pulses for a more homogeneous current distribution). After every pulse, the small diagonal current lines are used for probing the present state with a Hall measurement; an alternating probing current of 0.232 $\mathrm{mA_{RMS}}$ (equivalent to a current density of $\sim$0.0186 $\mathrm{A_{RMS}/\mu m^2}$) at 79 Hz is passed in one direction and the generated Hall voltage is detected along the perpendicular current line using standard lock-in techniques. Typically, there is a delay of 5 s between a pulse and the subsequent probing.

These experiments are performed within a cryostat, enabling the control of the temperature, that is placed in the center of a superconducting magnet, allowing for fields up to 16 T to be applied in the plane of the sample, along one of the probing lines (i.e., along the directions that are 45 ° rotated from the $\langle 11\overline{2}\rangle$ direction, approximately the $\langle \overline{0.7}\ 2.7\ \overline{2}\rangle$ and $\langle 2.7\ \overline{0.7}\ \overline{2}\rangle$ directions).

III. RESULTS AND DISCUSSION

A typical experimental result of electrical switching in the absence of a magnetic field is shown in Figs. 2(a) to 2(c). In the experiment, four current pulses are applied in one direction (I_1), whereafter four pulses are applied along the perpendicular direction (I_2). After each pulse, the Hall resistance R_t along the small diagonal current lines is measured; for better comparison between different devices and temperatures, we subtract the average Hall resistance $\overline{R}_t$ (averaged over the entire measurement) from the Hall resistance R_t and normalize the value to the longitudinal resistance R_0 (typically around 1.7 kΩ, but the exact value can differ between devices, measurements, and temperatures). Changes of the Néel vector should show up in the Hall resistance since one

of its contributions, the transverse component of the spin-Hall magnetoresistance (SMR), is sensitive to reorientations of the Néel vector of NiO from $+45^\circ$ to -45° with respect to the direction of the probing current [30]. It is observed that for a specific pulse current density ($0.89\,\mathrm{A}/\mu\mathrm{m}^2$) the two different pulse directions result in two distinct values of the Hall resistance, which is expected if indeed the Néel vector of NiO was switched by 90° by the current pulse. However, it should be noted that, as mentioned earlier, other nonmagnetic effects can give similar results.

A. Influence of current density

Upon increasing the pulse amplitude, as shown in Fig. 2(c), we find that the behavior changes from a step-like switching at $0.89\,\mathrm{A}/\mu\mathrm{m}^2$ to a sawtooth-like switching at $1.04\,\mathrm{A}/\mu\mathrm{m}^2$, where each subsequent current pulse in a certain direction still contributes to the final resistance state. This sawtooth-like switching behavior also has an inverted sign when compared to the step-like switching at lower current densities; for lower current density the pulses marked in green result in a high relative resistance state and the orange in a lower state, whereas for higher current density the green pulses result in a low resistance state and the orange in a higher state. For lower current densities [see Fig. 2(a) for $0.56\,\mathrm{A}/\mu\mathrm{m}^2$] the resistance state is insensitive to the direction of the pulses; for this current density, no switching behavior is observed.

The total current density-dependent switching behavior is summarized in Fig. 2(d), where the switching amplitude ΔR is plotted. This switching amplitude is defined as the difference between the (average) transverse resistance after a current pulse in either direction, i.e., $\Delta R = \overline{R}_{\mathrm{t,\,I_1}} - \overline{R}_{\mathrm{t,\,I_2}}$; for consistency between devices, all values are normalized by the longitudinal resistance of the device R_0. Here it becomes clear that starting from $0.5\,\mathrm{A}/\mu\mathrm{m}^2$ a form of current-induced switching becomes visible, reaching a maximum at around $0.9\,\mathrm{A}/\mu\mathrm{m}^2$. When the current density further increases, the switching amplitude starts to rapidly decrease, changes sign, and increases again (in the negative direction).

This switching behavior, with the change of sign and the associated transition from step-like to sawtooth-like switching indicates that there are at least two mechanisms at play in these experiments. As mentioned earlier, these mechanisms can be either magnetic or nonmagnetic of origin [16–18]. However, from this set of measurements alone it is impossible to tell if one of the mechanisms involved in the experiment is or is not magnetic of origin, and if so, which part of the curve is explained by this magnetic mechanism.

B. Electrical switching in high magnetic fields

To try to separate the magnetic from the nonmagnetic effects, we perform an identical experiment in a superconducting magnet where magnetic fields up to 16 T can be reached. When a sufficiently strong magnetic field is applied to the sample, the Néel vector (or equivalently, the individual magnetic moments) of the NiO layer will be forced in a configuration perpendicular to the magnetic field [21,31]. Note that this resembles the state after a spin-flop transition; however, thin films of NiO are known to rather undergo a monodomainization transition due to the relaxation of stress [21,32]. Upon applying a current pulse in such a magnetic field, we conjecture that one of two things will happen. One possibility is that the current pulse will not be sufficiently strong to overcome the external magnetic field and influence the orientation of the Néel vector. Alternatively, if the current pulse can affect the orientation of the Néel vector despite the presence of a strong external magnetic field, we expect the new orientation of the Néel vector will be reverted to the field-dominated orientation after the current pulse has stopped since the magnetic field is strong enough to force an orthogonal [33] orientation of the magnetic moments [21,31].

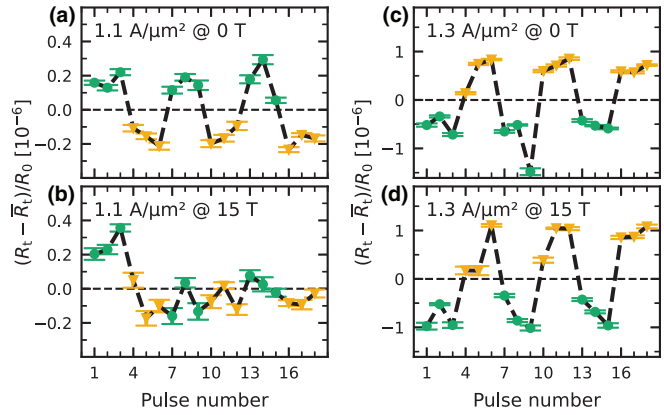

FIG. 3. Switching of NiO for multiple magnetic fields (top: 0 T; bottom: 15 T) and current pulse amplitudes (left: $1.1\,\mathrm{A}/\mu\mathrm{m}^2$; right: $1.3\,\mathrm{A}/\mu\mathrm{m}^2$) at 240 K. The green (orange) data points represent the resistance states (minus the average transverse resistance $\overline{R}_t$) after pulses in direction I_1 (I_2). All data are normalized by the longitudinal device resistance $R_0 = (1.74 \pm 0.01)\,\mathrm{k}\Omega$ and the black dashed lines are guides to the eye.

The results of these measurements are shown in Fig. 3, both for a medium current density [Figs. 3(a) and 3(b)] and for a higher current density [Figs. 3(c) and 3(d)]. Note that these measurements were performed at a different temperature (240 K rather than 250 K). Since both the magnetic and nonmagnetic effects are dependent on temperature [11], the exact current densities that are required to obtain the same switching patterns can differ between different temperatures. For this reduced temperature, a slightly higher current density is needed to obtain the same switching patterns as in Fig. 2; this is more thoroughly explored in the Supplemental Material [20].

Similar to the previous measurements (Fig. 2) we can see that the current pulses along the different directions (I_1 and I_2) result in a switching pattern. Please note that the high magnetic field setup results in a higher noise level in the measurements leading to a bit more irregular patterns than in the zero field; this has no impact on the conclusions of this work as these are based only on the general difference between the two current directions. When comparing the zero field experiment [Fig. 3(a)] to the high field experiment [15 T, Fig. 3(b)] for the medium current density, we observe that the switching behavior that is visible at zero field is absent for the high field experiment. For the high current density [Figs. 3(c)

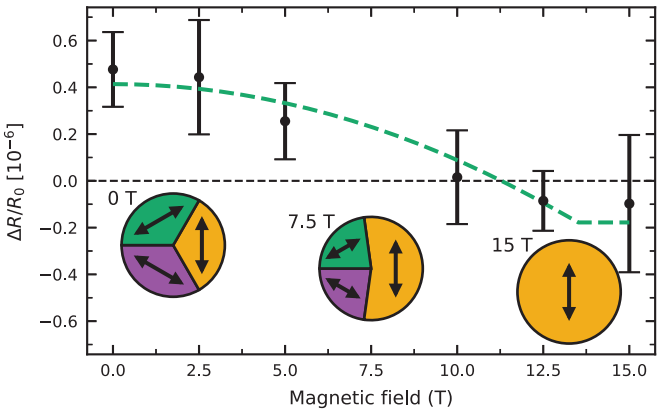

FIG. 4. Evolution of the switching amplitude as a function of the external magnetic fields at 240 K. The data points represent the measured switched states, averaged over every first pulse in that direction; the dashed green line represent the fitted magnetic field dependence Eq. (2). Due to the increased noise level in the high magnetic field setup, the standard deviation (error bars) for these measurements are relatively large; nevertheless, a clear field-dependent trend is visible. The pie charts represent the modeled distribution of the AF domains for 0 T, 7.5 T, and 15 T, from left to right; the arrows indicate the orientation of the magnetic moments in that domain.

and 3(d), respectively] no such trend is observed; for both zero and high magnetic fields, switching behavior is observed.

As the electrical switching of NiO is expected to be suppressed by a high magnetic field, we conjecture that the behavior we observe at medium current density is indeed caused by a magnetic effect; the switching behavior at higher current densities is then caused by nonmagnetic effects as these are not expected to be affected by the magnetic field. Note, however, that these two effects are not mutually exclusive and may have a gradual transition from one to the other. Hence, it is possible that in the high current density regime there is a small magnetic component and that in the medium current density regime there is a small nonmagnetic component.

To better identify these small contributions, we plot the switching amplitudes as a function of the external magnetic field magnitude in Fig. 4 for the medium current density. In this figure, the dependence of the switching amplitude on the external magnetic field is visible. At low magnetic fields, the switching amplitude is nearly unperturbed by the external magnetic field. However, towards higher magnetic fields the switching amplitude is greatly reduced until it reaches a plateau around ∼12 T.

C. Modeling the high-field switching behavior

We conjecture that this behavior demonstrates the presence of two entangled contributions, the magnetic one that gets suppressed by the high field and the nonmagnetic one that can be associated with the plateau that is reached at high fields. To substantiate this hypothesis, modeling of the population of the antiferromagnetic domains for NiO in high magnetic fields and the resulting SMR is needed; for this, we make use of the monodomainization model [21].

The model describes the NiO(111) layer of our samples by separating it into three domains where the Néel vectors of the three domains are separated by 120° (corresponding to the three spin domains in the NiO(111) plane [34]); in Fig. 4 this distribution is represented in pie charts. While this interpretation and the analytical expressions that are derived from the model are based on NiO(111) having three domains, the results are also valid in cases where the system has more (or equivalently, less well-defined) domains (see the Supplemental Material [20]), as is expected for the thin film of NiO in our samples [32].

In low magnetic fields, due to destressing, each of the domains takes up approximately an equal portion of the sample. When a strong magnetic field is applied, the distribution of these domains changes due to the Zeeman energy, where the domain with (the largest projection of) the Néel vector perpendicular to the external magnetic field are preferred; this domain will increase in size at the cost of the other domains. Finally, if the magnetic field surpasses the monodomainization field B_{md}, there is only a single domain left, namely, the domain with the Néel vector perpendicular to the external magnetic field.

This behavior results in a field-dependent transverse spin-Hall magnetoresistance (SMR) R_{SMR} that is given by [21]

$$R_{\mathrm{SMR}} \propto \begin{cases} \frac{B^2}{B_{\mathrm{md}}^2} & \text{if } B < B_{\mathrm{md}}, \\ 1 & \text{if } B \geqslant B_{\mathrm{md}}. \end{cases} \tag{1}$$

In the electrical switching experiments, it is expected that only a small portion of the magnetic structure is actually switched between the available domains upon applying a current pulse [32]. However, when an external magnetic field is applied and the distribution of domains changes, fewer domains are available to switch between. Therefore, we assume that the magnetic contribution to the switching signal scales as $R_{\mathrm{SMR,max}} - R_{\mathrm{SMR}}$. An additional field-independent offset R_{nm} was added to account for nonmagnetic effects that are expected to contribute to the measured switching amplitude. When combined with Eq. 1, the switching amplitude can then be expressed as

$$\Delta R = \begin{cases} R_{\mathrm{nm}} - R_{\mathrm{m}}\left(1 - \frac{B^2}{B_{\mathrm{md}}^2}\right) & \text{if } B < B_{\mathrm{md}}, \\ R_{\mathrm{nm}} & \text{if } B \geqslant B_{\mathrm{md}}, \end{cases} \tag{2}$$

where R_{m} is the SMR proportionality constant that accounts for the contribution of the changes in the antiferromagnetic state to the measured switching amplitude.

To fit the model to the data, the monodomainization field $B_{\mathrm{md}} = 13.5$ T [20] is kept constant and only R_{m} and R_{nm} are varied. As shown in Fig. 4, the fitted curve follows the data closely and emphasizes the gradual suppression of the magnetic contribution up to the monodomainization field and the nonmagnetic plateau for higher fields.

D. Disentangling magnetic and nonmagnetic effects

As we now understand the field dependence of the switching amplitude ΔR, it can be used to help settle the debate regarding the contributions of the magnetic and nonmagnetic, parasitic effects to the observed switching signal. To directly connect to the earlier discussed current dependence (Fig. 2),

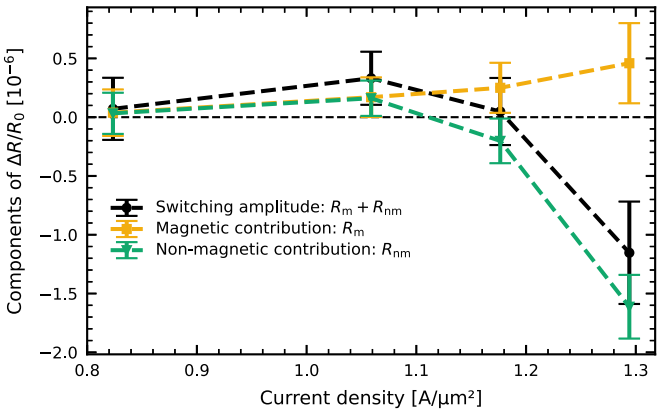

FIG. 5. Separated magnetic (orange) and nonmagnetic (green) contributions to the electrical switching experiments as a function of pulse current density at 240 K. The two contributions were extracted from the magnetic field dependence of the switching amplitude for each current density by fitting the data with Eq. (2) for R_m and R_{nm}. The full switching amplitude (black circular marks) is the sum of R_m and R_{nm} and can be compared to the switching amplitude in Fig. 2(d).

we repeat the switching in high magnetic field experiments for a series of current densities. By fitting the monodomainization model [Eq. 2] to the measurements at every current density, a measure for both the magnetic (R_m) and the nonmagnetic (R_{nm}) contribution to the signal at zero magnetic field can be obtained.

In Fig. 5 these separate contributions are plotted as a function of the current density of the pulses. Here, it can be noted that the magnetic component slowly increases with increasing current density. Simultaneously it is observed that the nonmagnetic part rises (with an opposite sign from the magnetic part) from 0.8 A/μm^2 to ∼1.05 A/μm^2; for higher current densities, however, it changes sign and the magnitude rises strongly in a nonlinear manner, which hints at a thermal origin of this effect [11].

The sum of the two contributions shows (qualitatively) the same behavior as the switching amplitude at zero magnetic field [Fig. 2(d)], despite a small mismatch in temperature [250 K for Fig. 2(d) compared to 240 K for Fig. 5, related to different temperature control possibilities in the different setups]. For medium current densities, this indicates that the observed (step-like) switching signal [e.g., Fig. 2(b)] is a combination of both magnetic and nonmagnetic components. At high current densities [e.g., Fig. 2(c)], the (sawtooth-like) switching signal is mostly a result of the nonmagnetic contributions; the inverted sign of this switching signal is also a consequence of these nonmagnetic effects. These conclusions are in line with earlier interpretations [12,14] that the step-like switching can often be attributed to magnetic effects and sawtooth-like switching to nonmagnetic effects.

We are convinced—in particular, based on the agreement with the expected behavior and the high magnetic field, typical for antiferromagnetic NiO, needed to suppress the switching—that these results show that we are indeed able to separate the magnetic and nonmagnetic effects using high magnetic fields. Additional control experiments could be performed to further support these conclusions; to enable a meaningful comparison with the present data, a careful detailed analysis of results from nonmagnetic control samples would be required.

IV. CONCLUSION

In summary, we investigated the field dependence of the electrical switching of NiO to distinguish between the magnetic and nonmagnetic contributions to the electrical switching experiments. We showed that for lower current densities the (step-like) switching pattern was greatly suppressed upon applying a high magnetic field. For higher current densities, on the other hand, the (inverted, sawtooth-like) switching pattern remained largely unaffected by the magnetic field, hinting at a nonmagnetic origin.

Using a monodomainization model the magnetic and nonmagnetic contributions can be separated from each other. This confirmed that the switching at lower current densities is, in part, due to actual magnetic switching of NiO; however, also at these lower current densities, a nonmagnetic contribution is present. Moreover, it showed that the change-of-sign that is observed at higher current densities is caused by no-magnetic effects; for these higher current densities there was still a magnetic part (which was slightly stronger than the magnetic effects at lower current densities), but the nonmagnetic component dominated the signal.

We showed that a strong magnetic field can be used to quantitatively disentangle magnetic and nonmagnetic effects in experiments aimed at the electrical switching experiments of antiferromagnets. This technique relieves the necessity for imaging the antiferromagnetic structure as a way to study the electrical switching of antiferromagnets and thereby opens a way to investigate more complex devices where the antiferromagnetic layer is just one of the many layers and imaging of the antiferromagnetic domains becomes increasingly difficult or impossible.

ACKNOWLEDGMENTS

We acknowledge S. Peeters for measuring the sheet resistance of an unpatterned sample. Sample fabrication was performed using the NanoLabNL facilities. The research performed here was funded by the Dutch Research Council (NWO) under Grant No. 680-91-113. This work was supported by HFML-RU/NWO-I, member of the European Magnetic Field Laboratory (EMFL). C.F.S. and M.J.G. conceived the experiments, fabricated the samples with help from T.J.K., and performed the measurements while advised by H.J.M.S. High magnetic field experiments were performed by C.F.S. and M.J.G. with help from K.R. and M.E.B. while advised by U.Z. C.F.S. performed the data analysis while advised by M.J.G., H.J.M.S., and R.D.

[1] T. Jungwirth, X. Marti, P. Wadley, and J. Wunderlich, Antiferromagnetic spintronics, Nat. Nanotechnol. **11**, 231 (2016).

[2] R. Khymyn, I. Lisenkov, V. Tiberkevich, B. A. Ivanov, and A. Slavin, Antiferromagnetic THz-frequency Josephson-like oscillator driven by spin current, Sci. Rep. **7**, 43705 (2017).

[3] P. Stremoukhov, A. Safin, M. Logunov, S. Nikitov, and A. Kirilyuk, Spintronic terahertz-frequency nonlinear emitter based on the canted antiferromagnet-platinum bilayers, J. Appl. Phys. **125**, 223903 (2019).

[4] R. Cheng, D. Xiao, and A. Brataas, Terahertz Antiferromagnetic Spin Hall Nano-Oscillator, Phys. Rev. Lett. **116**, 207603 (2016).

[5] P. Wadley, B. Howells, J. Železný, C. Andrews, V. Hills, R. P. Campion, V. Novák, K. Olejník, F. Maccherozzi, S. S. Dhesi, S. Y. Martin, T. Wagner, J. Wunderlich, F. Freimuth, Y. Mokrousov, J. Kuneš, J. S. Chauhan, M. J. Grzybowski, A. W. Rushforth, K. W. Edmonds *et al.*, Electrical switching of an antiferromagnet, Science **351**, 587 (2016).

[6] X. Z. Chen, R. Zarzuela, J. Zhang, C. Song, X. F. Zhou, G. Y. Shi, F. Li, H. A. Zhou, W. J. Jiang, F. Pan, and Y. Tserkovnyak, Antidamping-Torque-Induced Switching in Biaxial Antiferromagnetic Insulators, Phys. Rev. Lett. **120**, 207204 (2018).

[7] Y. Li, J. Liang, H. Yang, H. Zheng, and K. Wang, Current-induced out-of-plane effective magnetic field in antiferromagnet/heavy metal/ferromagnet/heavy metal multilayer, Appl. Phys. Lett. **117**, 092404 (2020).

[8] X. H. Liu, K. W. Edmonds, Z. P. Zhou, and K. Y. Wang, Tuning Interfacial Spins in Antiferromagnetic–Ferromagnetic–Heavy-Metal Heterostructures via Spin-Orbit Torque, Phys. Rev. Appl. **13**, 014059 (2020).

[9] H. Tsai, T. Higo, K. Kondou, T. Nomoto, A. Sakai, A. Kobayashi, T. Nakano, K. Yakushiji, R. Arita, S. Miwa, Y. Otani, and S. Nakatsuji, Electrical manipulation of a topological antiferromagnetic state, Nature (London) **580**, 608 (2020).

[10] Y. Deng, R. Li, and X. Liu, Thickness dependent anomalous Hall effect in noncollinear antiferromagnetic Mn_3Sn polycrystalline thin films, J. Alloys Compd. **874**, 159910 (2021).

[11] M. J. Grzybowski, C. F. Schippers, M. E. Bal, K. Rubi, U. Zeitler, M. Foltyn, B. Koopmans, and H. J. M. Swagten, Electrical switching of antiferromagnetic CoO|Pt across the Néel temperature, Appl. Phys. Lett. **120**, 122405 (2022).

[12] Y. Cheng, S. Yu, M. Zhu, J. Hwang, and F. Yang, Electrical Switching of Tristate Antiferromagnetic Néel order in α-Fe_2O_3 Epitaxial Films, Phys. Rev. Lett. **124**, 027202 (2020).

[13] T. Moriyama, K. Oda, T. Ohkochi, M. Kimata, and T. Ono, Spin torque control of antiferromagnetic moments in NiO, Sci. Rep. **8**, 14167 (2018).

[14] L. Baldrati, O. Gomonay, A. Ross, M. Filianina, R. Lebrun, R. Ramos, C. Leveille, F. Fuhrmann, T. R. Forrest, F. Maccherozzi, S. Valencia, F. Kronast, E. Saitoh, J. Sinova, and M. Kläui, Mechanism of Néel Order Switching in Antiferromagnetic Thin Films Revealed by Magnetotransport and Direct Imaging, Phys. Rev. Lett. **123**, 177201 (2019).

[15] H. Meer, F. Schreiber, C. Schmitt, R. Ramos, E. Saitoh, O. Gomonay, J. Sinova, L. Baldrati, and M. Kläui, Direct imaging of current-induced antiferromagnetic switching revealing a pure thermomagnetoelastic switching mechanism in NiO, Nano Lett. **21**, 114 (2021).

[16] C. C. Chiang, S. Y. Huang, D. Qu, P. H. Wu, and C. L. Chien, Absence of Evidence of Electrical Switching of the Antiferromagnetic Néel Vector, Phys. Rev. Lett. **123**, 227203 (2019).

[17] A. Churikova, D. Bono, B. Neltner, A. Wittmann, L. Scipioni, A. Shepard, T. Newhouse-Illige, J. Greer, and G. S. D. Beach, Non-magnetic origin of spin Hall magnetoresistance-like signals in Pt films and epitaxial NiO/Pt bilayers, Appl. Phys. Lett. **116**, 022410 (2020).

[18] T. Matalla-Wagner, J.-M. Schmalhorst, G. Reiss, N. Tamura, and M. Meinert, Resistive contribution in electrical-switching experiments with antiferromagnets, Phys. Rev. Res. **2**, 033077 (2020).

[19] P. Wadley, S. Reimers, M. J. Grzybowski, C. Andrews, M. Wang, J. S. Chauhan, B. L. Gallagher, R. P. Campion, K. W. Edmonds, S. S. Dhesi, F. Maccherozzi, V. Novak, J. Wunderlich, and T. Jungwirth, Current polarity-dependent manipulation of antiferromagnetic domains, Nat. Nanotechnol. **13**, 362 (2018).

[20] See Supplemental Material at http://link.aps.org/supplemental/10.1103/PhysRevB.106.174434 for details on growth and characterization of the samples used in this work, the determination of the monodomainization field of the NiO samples, the validation of the monodomainization model for thin films of NiO, and the temperature dependence of the switching amplitude.

[21] J. Fischer, O. Gomonay, R. Schlitz, K. Ganzhorn, N. Vlietstra, M. Althammer, H. Huebl, M. Opel, R. Gross, S. T. B. Goennenwein, and S. Geprägs, Spin Hall magnetoresistance in antiferromagnet/heavy-metal heterostructures, Phys. Rev. B **97**, 014417 (2018).

[22] M. Kimata, T. Moriyama, K. Oda, and T. Ono, Distinct domain reversal mechanisms in epitaxial and polycrystalline antiferromagnetic NiO films from high-field spin Hall magnetoresistance, Appl. Phys. Lett. **116**, 192402 (2020).

[23] A. N. Mansour, Characterization of NiO by XPS, Surf. Sci. Spectra **3**, 231 (1994).

[24] F. M. Smits, Measurement of sheet resistivities with the four-point probe, Bell Syst. Tech. J. **37**, 711 (1958).

[25] J. W. Arblaster, Selected electrical resistivity values for the platinum group of metals part I: Palladium and platinum, Johnson Matthey Technol. Rev. **59**, 174 (2015).

[26] C. T. Boone, J. M. Shaw, H. T. Nembach, and T. J. Silva, Spin-scattering rates in metallic thin films measured by ferromagnetic resonance damping enhanced by spin-pumping, J. Appl. Phys. **117**, 223910 (2015).

[27] M.-H. Nguyen, D. C. Ralph, and R. A. Buhrman, Spin Torque Study of the Spin Hall Conductivity and Spin Diffusion Length in Platinum Thin Films with Varying Resistivity, Phys. Rev. Lett. **116**, 126601 (2016).

[28] A. Khamkongkaeo, N. Mothaneeyachart, P. Sriwattana, T. Boonchuduang, T. Phetrattanarangsi, C. Thongchai, B. Sakkomolsri, A. Pimsawat, S. Daengsakul, S. Phumying, N. Chanlek, P. Kidkhunthod, and B. Lohwongwatana, Ferromagnetism and diamagnetism behaviors of MgO synthesized via thermal decomposition method, J. Alloys Compd. **705**, 668 (2017).

[29] M. M. Lacerda, F. Kargar, E. Aytan, R. Samnakay, B. Debnath, J. X. Li, A. Khitun, R. K. Lake, J. Shi, and A. A. Balandin, Variable-temperature inelastic light scattering spectroscopy of nickel oxide: Disentangling phonons and magnons, Appl. Phys. Lett. **110**, 202406 (2017).

[30] Y.-T. Chen, S. Takahashi, H. Nakayama, M. Althammer, S. T. B. Goennenwein, E. Saitoh, and G. E. W. Bauer, Theory of spin Hall magnetoresistance (SMR) and related phenomena, J. Phys.: Condens. Matter **28**, 103004 (2016).

[31] F. L. A. Machado, P. R. T. Ribeiro, J. Holanda, R. L. Rodríguez-Suárez, A. Azevedo, and S. M. Rezende, Spin-flop transition in the easy-plane antiferromagnet nickel oxide, Phys. Rev. B **95**, 104418 (2017).

[32] I. Gray, T. Moriyama, N. Sivadas, G. M. Stiehl, J. T. Heron, R. Need, B. J. Kirby, D. H. Low, K. C. Nowack, D. G. Schlom, D. C. Ralph, T. Ono, and G. D. Fuchs, Spin Seebeck Imaging of Spin-Torque Switching in Antiferromagnetic Pt/NiO Heterostructures, Phys. Rev. X **9**, 041016 (2019).

[33] Although the high magnetic fields that are used in these experiments are expected to cant the magnetic moments slightly away from a direction that is perfectly orthogonal to the external magnetic field, we estimate that this canting is sufficiently small ($\sim 0.4^\circ$ at 15 T) that this deviation can be disregarded in the interpretation of the experiments.

[34] E. Uchida, N. Fukuoka, H. Kondoh, T. Takeda, Y. Nakazumi, and T. Nagamiya, Magnetic anisotropy of single crystals of NiO and MnO, J. Phys. Soc. Jpn. **23**, 1197 (1967).